

## Supplementary Material

### An L-cysteine based sensor for Cu<sup>2+</sup> detection applicable for both environmental water and human plasma

Yanhong Chen<sup>a</sup>, Li Lv<sup>a,\*</sup>, Xuanjiao Mao<sup>b</sup>, Jun Chai<sup>a</sup>, Jayne Wu<sup>c</sup>, Yicheng Zhou<sup>a</sup>, Jian Zhang<sup>a</sup>, Haochen Qi<sup>a,\*</sup>

<sup>a</sup> College of Electrical and Electronic Engineering, Wenzhou University, Wenzhou 325035, China

<sup>b</sup> Clinical Laboratory, The People's Hospital of Pingyang, Wenzhou 325400, China

<sup>c</sup> Department of Electrical Engineering and Computer Science, The University of Tennessee, Knoxville, TN 37996, USA

<sup>d</sup> State Key Laboratory of Transducer Technology, Shanghai Institute of Microsystem and Information Technology, Chinese Academy of Sciences, Shanghai 200050, China

### Table of Contents

Fig. S1 CV curves of SPCE cleaning step (pretreatment for SPCEs).

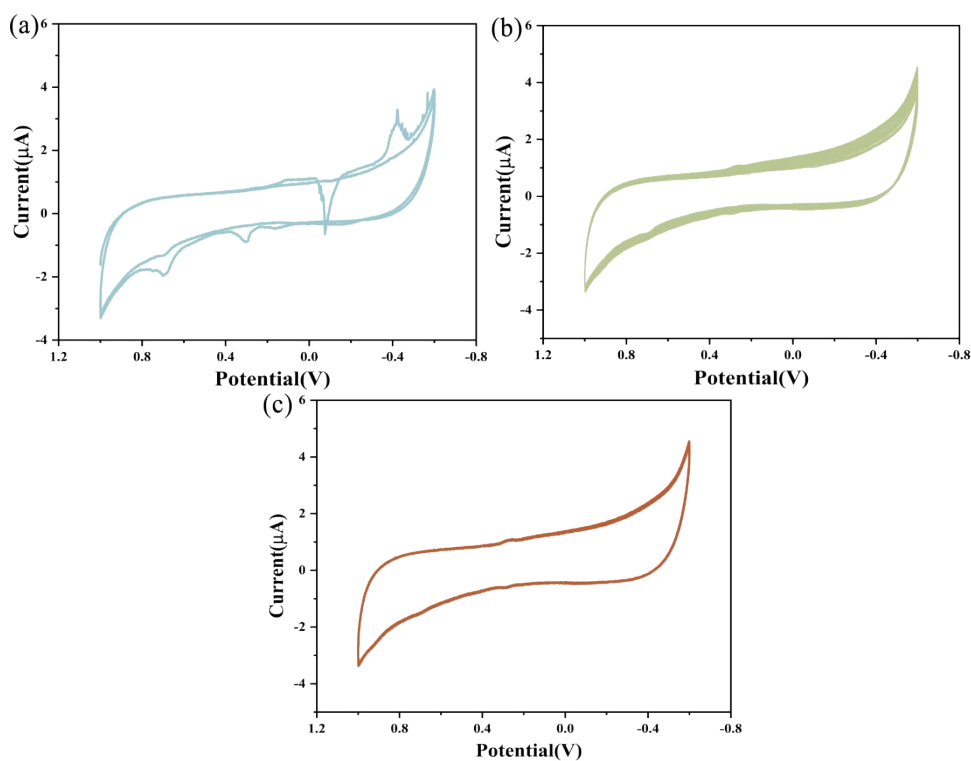
Fig. S2 Electrodeposition process of AuNPs.

Fig. S3 Functional characterization of sensors.

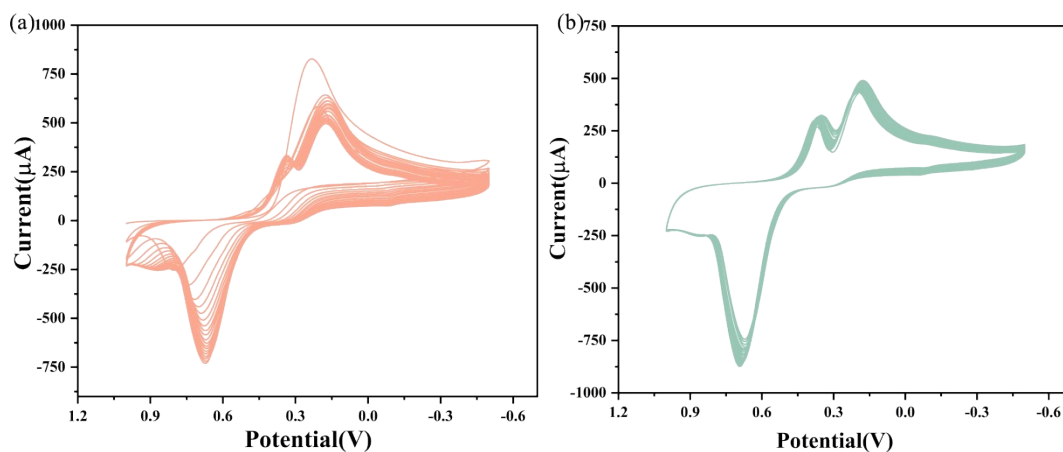
Fig. S4 Optimization of background PH value and enrichment time.

Fig. S5 Reproducibility and stability of the sensor.

Fig. S6 DPV curve and fitting curve for determination of Cu<sup>2+</sup> in plasma



**Fig. S1 CV curves of cleaning step (a) CV curves for the first four stages of the cleaning step, (b) CV curves for the last 28 stages of the cleaning step, (c) CV curves for the last 4 stages of the cleaning step**



**Fig. S2 CV electrodeposition of AuNPs (a) CV scanning results of the first 36 stages of AuNPs electrodeposition, (b) CV scanning results of AuNP electrodeposition at the last 36 stages**

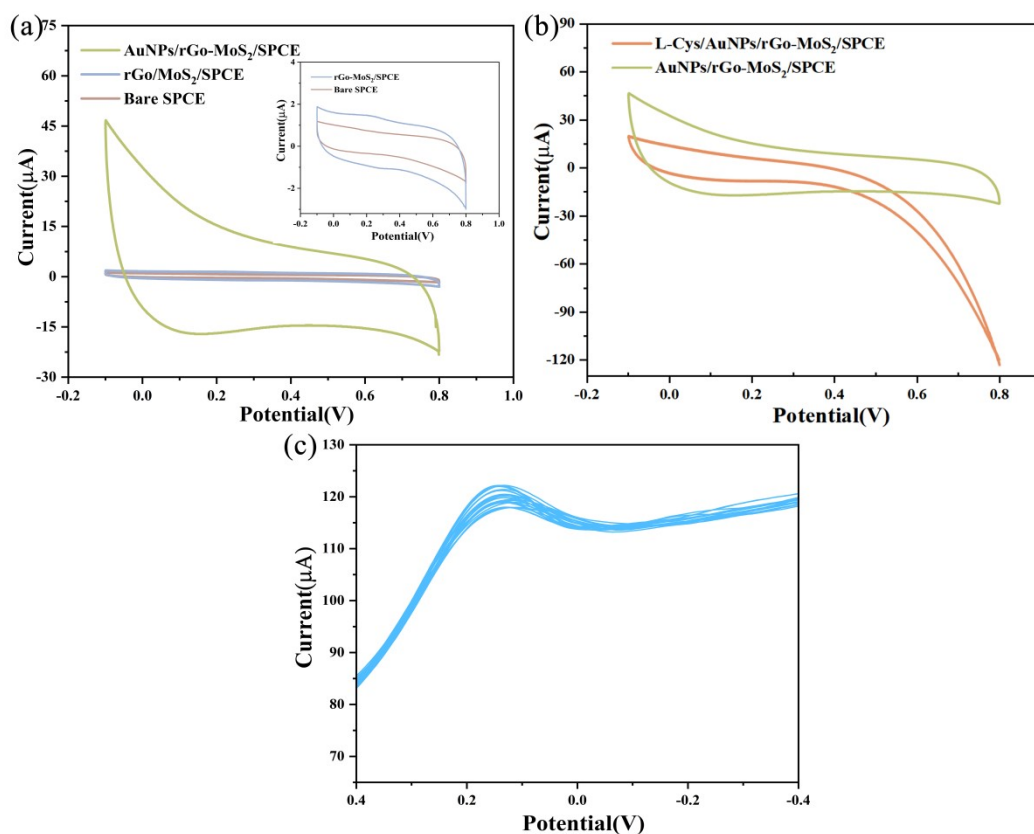


**Fig. S3 (a)CV curves from a bare SPCE, rGo-MoS<sub>2</sub>/SPCE and AuNPs/rGo-MoS<sub>2</sub>/SPCE, (b) AuNPs/rGo-MoS<sub>2</sub> / SPCE and L-Cys/AuNPs/rGo-MoS<sub>2</sub> / SPCE, (c)DPV curves for 30 measurements of 60 μL of 50 μM Cu<sup>2+</sup> by L-Cys/AuNPs/rGo-MoS<sub>2</sub>/SPCE**

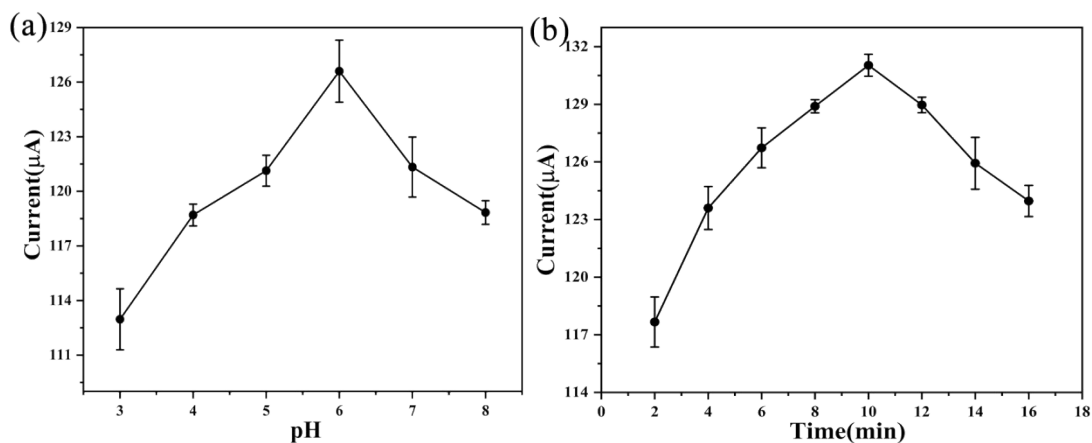


**Fig. S4 (a) Optimization of PH of the background (0.1 × PBS), (b) Optimization of Cu<sup>2+</sup> enrichment time**

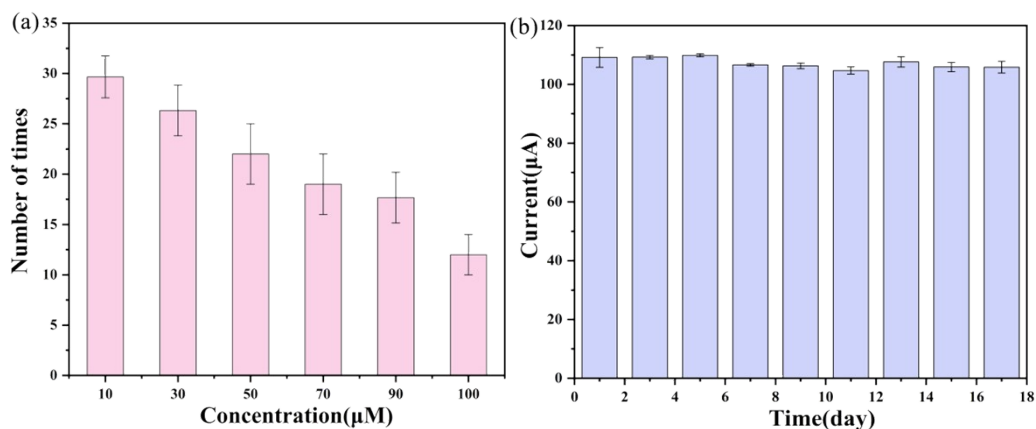


**Fig. S5 (a) Scan number of DPV peak current from six concentrations of  $\text{Cu}^{2+}$  using three sensors for each concentration, (b) DPV peak current from the sensors after being stored at 4 °C for different days, with the  $\text{Cu}^{2+}$  concentration of 50  $\mu\text{M}$**

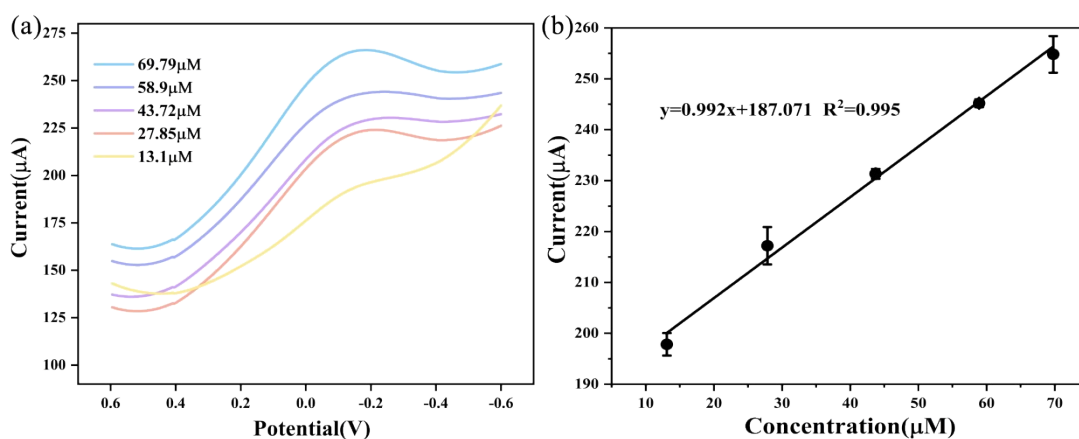


**Fig. S6 (a) DPV curves from spiked  $\text{Cu}^{2+}$  in plasma, (b) calibrated curve of the peak current for  $\text{Cu}^{2+}$  detection in plasma**

**Table S1 DPV peak potential and peak current for 30 measurements of 60  $\mu\text{L}$  of 50  $\mu\text{M}$   $\text{Cu}^{2+}$  by L-Cys/AuNPs/rGo-MoS<sub>2</sub> / SPCE**

Number of times	Peak potential/V	Peak current/ $\mu\text{A}$
1	0.150	123
2	0.150	122
3	0.150	121
4	0.150	121
5	0.150	121
6	0.145	121

---

7	0.150	121
8	0.150	121
9	0.150	120
10	0.150	120
11	0.150	122
12	0.145	122
13	0.150	121
14	0.140	121
15	0.145	121
16	0.150	119
17	0.150	120
18	0.150	120
19	0.150	120
20	0.130	119
21	0.140	119
22	0.140	119
23	0.140	118
24	0.135	118
25	0.125	119
26	0.135	119
27	0.135	119
28	0.130	118
29	0.130	118
30	0.130	119

---